Proton Transfer in the Enzyme Carbonic Anhydrase: An *ab Initio* Study

Dongsheng Lu and Gregory A. Voth*

Contribution from the Department of Chemistry and Henry Eyring Center for Theoretical Chemistry, University of Utah, Salt Lake City, Utah 84112

Received September 29, 1997

Abstract: *Ab initio* calculations have been performed to probe possible proton-transfer pathways in carbonic anhydrase. It is found that the proton transfer in the dehydration direction involves an energy barrier of around 8−10 kcal/mol, which agrees well with experiment, while the proton-transfer barrier in the hydration (away from zinc) direction is sensitive to the histidine ligand bonding around the Zn ion. The water ligand dependence of the proton-transfer energy barrier reveals a requirement of certain hydrogen bond formation in the active site. Preliminary studies involving two and three proton transfers through hydrogen-bonded water chains show that the donor−acceptor distance and the water chain motion are crucial to the proton-transfer energetics. On the basis of these results, a picture of the proton-transfer energetics and mechanism is presented and the effect of the His-64 ligand on the process is discussed.

Introduction

Carbonic anhydrase (CA) is a zinc-containing enzyme which catalyzes the conversion between CO_2 and HCO_3^-, i.e.,

$$CO_2 + H_2O \rightleftharpoons HCO_3^- + H^+ \quad (1)$$

The catalytic mechanism of CA has been subject to extensive study, both experimentally[1−19] and theoretically,[22−28] over a period of decades. It is now generally accepted that the catalytic mechanism consists of two steps: The first step (eq 2 below) involves the proton release from Zn-bound water to form Zn-bound hydroxide, while the second step (eq 3 below) involves nucleophilic attack of CO_2 with Zn-bound hydroxide to form HCO_3^-, which subsequently leaves the active site. These two steps are:

$$EZnOH_2 \rightleftharpoons EZnOH^- + H^+ \quad (2)$$

$$EZnOH^- + CO_2 \rightleftharpoons EZnHCO_3^-$$

$$EZnHCO_3^- + H_2O \rightleftharpoons EZnH_2O + HCO_3^- \quad (3)$$

Here "E" stands for the enzyme. After the completion of the second step, the next cycle starts and begins the reaction of another CO_2 molecule. Experiments on solvent hydrogen isotope effects[4,7] and the release rate of ^{18}O-labeled water into solvent at different buffer concentrations[8] have shown that the proton transfer (PT) of eq 2 is the rate-limiting step of the maximal velocity at high buffer concentrations. At low buffer concentrations, the proton release into the medium is rate-limiting.[17]

(1) Earnhardt, J. N.; Silverman, D. N. In *Comprehensive Biological Catalysis*; Sinnott, M., Ed.; Academic Press: 1998; pp 483−506.
(2) Christianson, D. W.; Fierke, C. A. *Acc. Chem. Res.* **1996**, *29*, 331 and references therein.
(3) Lindskog, S. *Pharmacol. Ther.* **1997**, *74*, 1.
(4) Steiner, H.; Jonsson, B. H.; Lindskog, S. *Eur. J. Biochem.* **1975**, *59*, 253.
(5) (a) Lindskog, S.; Engberg, P.; Forsman, C.; Ibrahim, S. A.; Jonsson, B. H.; Simonsson, I.; Tibell, L. *Ann. N.Y. Acad. Sci.* **1984**, *429*, 61. (b) Lindskog, S. In *Zinc Enzymes*; Spiro, T. G., Ed.; Wiley: New York, 1983; pp 78−121. (c)Lindskog, S.; Coleman, J. E. *Proc. Natl. Acad. Sci. U.S.A.* **1973**, *70*, 2505.
(6) Silverman, D. N.; Lindskog, S. *Acc. Chem. Res.* **1988**, *21*, 30.
(7) Pocker, Y.; Bjorkquist, D. W. *Biochemistry* **1977**, *16*, 5698.
(8) (a) Silverman, D. N.; Tu, C. K.; Lindskog, S.; Wynns, G. C. *J. Am. Chem. Soc.* **1979**, *101*, 6734. (b) Tu, C. K.; Silverman, D. N. *J. Am. Chem. Soc.* **1975**, *97*, 5935.
(9) Silverman, D. N.; Tu, C. K.; Chen, X.; Tanhouser, S. M.; Kresge, A. J.; Laipis, P. J. *Biochemistry* **1993**, *32*, 10757.
(10) Tu, C. K.; Silverman, D. N. *Biochemistry* **1985**, *24*, 5881.
(11) (a) Fierke, C. A.; Calderone, T. L.; Krebs, J. F. *Biochemistry* **1991**, *30*, 11054. (b) Kiefer, L. L.; Paterno, S. A.; Fierke, C. A. *J. Am. Chem. Soc.* **1995**, *117*, 6831.
(12) Ghannam, A. F.; Tsen, W.; Rowlett, R. S. *J. Biol. Chem.* **1986**, *261*, 1164.
(13) Lesburg, C. A.; Christianson, D. W. *J. Am. Chem. Soc.* **1995**, *117*, 6838.
(14) Nair, S. K.; Christianson, D. W. *J. Am. Chem. Soc.* **1991**, *117*, 9455.
(15) Kannan, K. K.; Ramanadham, M.; Jones, T. A. *Ann. N.Y. Acad. Sci.* **1984**, *429*, 49.
(16) Gothe P. O.; Nyman, P. O. *FEBS Lett.* **1972**, *21*, 159.
(17) Lindskog, S.; Behravan, G.; Engstrant, C.; Forsman, C.; Jonsson, B.; Liang, Z.; Ren, X.; Xu e, Y. In *Carbonic Anhydrase: From Biochemistry and Genetics to Physiology and Clinical Medicine*; Botre, F., Gros, G., Storey, B. T., Eds.; VCH: Weinheim, 1991; pp 1−13.
(18) Pocker, Y.; Janjic, N.; Miao, C. H. In *Zinc Enzymes*; Bertini, I., Luchinat, C., Maret, W., Zeppezauer, M., Eds.; Birkhäuser: Boston, 1986; pp 341−356.
(19) Tu, C. K.; Wynns, G. C.; Silverman, D. N. *J. Biol. Chem.* **1981**, *256*, 9466.
(20) Heck, R. W.; Boriack-Sjodin, P. A.; Qian, M.; Tu, C.; Christianson, D. W.; Laipis, P. J. and Silverman, D. N. *Biochemistry* **1996**, *35*, 11605.
(21) Christianson, D. W. *Rigaku Journal* **1996**, *13*, 8.
(22) (a) Liang, J.; Lipscomb, W. N. *Biochemistry* **1988**, *27*, 8797; (b) *Biochemistry* **1987**, *26*, 5293; (c) *J. Am. Chem. Soc.* **1986**, *108*, 5051. (d) Lipscomb, W. N. *Annu. Rev. Biochem.* **1983**, *52*, 17. (e) Liang, J.; Lipscomb, W. N. *Int. J. Quantum. Chem.* **1989**, *36*, 299.
(23) (a) Jacob, O.; Cardenas, R.; Tapia, O. *J. Am. Chem. Soc.* **1990**, *112*, 8692. (b) Jacob, O.; Tapia, O. *Int. J. Quantum Chem.* **1992**, *42*, 1271.
(24) (a) Merz, K. M., Jr.; Hoffmann, R.; Dewar, M. J. S. *J. Am. Chem. Soc.* **1989**, *111*, 5636. (b) Merz, K. M., Jr. *J. Am. Chem. Soc.* **1990**, *112*, 7973; (c) *J. Am. Chem. Soc.* **1991**, *113*, 406; (d) *J. Am. Chem. Soc.* **1991**, *113*, 3572. (e) Zheng Y.; Merz, K. M., Jr. *J. Am. Chem. Soc.* **1992**, *114*, 10498 and references therein.
(25) Åqvist, A.; Warshel, A. *J. Mol. Biol.* **1992**, *224*, 7.
(26) Merz, K. M. *J. Am. Chem. Soc.* **1991**, *113*, 3572.
(27) (a) Demoulin D.; Pullman, A. *Theor. Chim. Acta* **1978**, *49*, 161. (b) Pullman A.; Demoulin, D. *Intl. J. Quantum Chem.* **1979**, *16*, 641.
(28) Sheridan, R. P.; Allen, L. C. *J. Am. Chem. Soc.* **1981**, *103*, 1544.

S0002-7863(97)03397-0 CCC: $15.00
Published on Web 04/14/1998

Despite the general agreement about the chemical mechanism involved in the catalytic process [eqs 2 and 3], the picture of the proton-transfer mechanism and its dynamics is somewhat unresolved. Extensive experimental studies by Silverman and Linskog[6] support the idea of an intramolecular proton shuttle between a Zn-bound water and the His-64 group, which was originally proposed by Steiner et al.[4] X-ray diffraction results[13] show that this proposal is feasible: the Zn^{2+} ion is found to be around 7.8 Å away from His-64, so between them are possibly as many as three water molecules which could form a bridge necessary for a proton shuttle. Studies on the pK_a of functional groups in the active site also support this mechanism: the Zn-bound water has about the same pK_a (∼7) as protonated His-64. This is rather important to the mutual proton exchange since a large difference in pK_a could lead to a significant barrier in one of the proton-transfer directions. This requirement has excluded the possibility of a proton-transfer role by other functional groups or residues.[26] The most recent studies on the CA V isozyme also support the proton-transfer mechanism outlined above.[20,21] Several recent reviews[1−3] provide a complete description of the current state of experimental affairs for CA.

On the basis of the experimental facts, one may rightly conclude that His-64 is likely to play an important role in the catalytic process in CA. However, the specific manner in which His-64 participates in the proton transfer is still not resolved. The basic issue is how the proton transfer occurs between Zn-bound water and His-64 if the mechanism suggested by Steiner et al.[4] is correct. If this process involves a large energy barrier, it would cast doubt on the role of His-64 in the catalytic process. Theoretical studies can help to resolve these issues, but to date, there has been limited theoretical input.[22,24,25] Liang and Lipscomb[22] carried out a large number of calculations using semiempirical (PRDDO) methods. They considered the proton transfer in the hydration direction between a Zn-bound water and an ammonia molecule under a variety of situations. While the trend of the proton-transfer energetics under various situations (e.g., with different numbers of ligand ammonia molecules or different numbers of bridge water molecules) may be correct, their calculations cannot be considered quantitative. For example, a value of 30 kcal/mol was obtained for the hydration direction PT barrier, as compared to 7.8 kcal/mol from kinetic experimental measurements, and 8−10 kcal/mol on the basis of pK_a considerations. The authors ascribed this difference to basis set error and correlation effects. Merz et al.[24] also studied the deprotonation of Zn-bound water using the semiempirical AM1 method. They considered the proton relay from Zn-bound water to an imidazole molecule. Their deprotonation energy is also too high (23 kcal/mol) in comparison with experiment. Thus, better *ab initio* calculations are needed to quantify the proton shuttle mechanism, and this is the primary goal of the present paper.

In the previous theoretical calculations, the three histidine ligands around the Zn^{2+} ion were also modeled as water and/or ammonia molecules. Apart from the stereochemical considerations which might have a significant effect on the energetics of the various processes, the difference in the Zn^{2+} and proton affinity of water, ammonia, and imidazole molecules will also have an important effect on the pK_a of Zn-bound water. As will be shown in later sections, the distance between the Zn^{2+} ion and the donor water oxygen differs by 0.15 Å as the ligands are changed from imidazole to ammonia and/or water molecules, while the energy barrier can vary by more than 10 kcal/mol. These results demonstrate that the assumption of replacing imidazole ligands with ammonia molecules, which has been used widely after the lead of Pullman and co-workers,[27] is not likely to be quantitatively valid.

It is also worth mentioning that, by using a purely classical model transferred from the fitting of Zn^{2+} hydration energy and radial distribution functions, Åqvist and Warshel[25] obtained a reasonable estimate of the effect of Zn^{2+} in lowering the PT barrier for the Zn-bound water in CA. Their approach, which is based on an empirical potential, gives a good fit to the 6-fold-coordinated Zn^{2+} ion in aqueous solution. However, the transferability of this model to the 4-fold-coordinated site in CA is not obvious. Furthermore, as the proton-transfer barrier is very sensitive to the ligand environment around the Zn^{2+} ion as will be shown later, the results obtained by Åqvist and Warshel may be somewhat fortuitous.

In the present paper, extensive calculations will be presented for the proton-transfer reactions relevant to CA using a more accurate *ab initio* treatment, as described in the next section. This method is first shown to perform well for the calculation of the energy barriers for a number of calibration reactions. Then, the PT energy surface will be explored and shown to give a more complicated situation than a simple transition state. To be specific, the PT energy barrier is found to be dynamically related to the proton and donor (D)−acceptor (A) motions. Depending on this coupling, the barrier height varies significantly. Although even more accurate dynamical simulations are desirable, the present calculations show that *ab initio* results for the PT barriers in the dehydration and hydration directions agree rather well with experiment, and support the mechanism of a proton transfer between Zn-bound water and His-64 involving a water shuttle.

Ab Initio Methodology and Calibration

Proton transfer in CA in both the hydration (away from zinc) and dehydration directions will be considered in this paper under various conditions. For donor species "D" and acceptor species "A", the potential curves are calculated as a function of R(DA) and r(DH) or r(DH) − R(DA)/2, depending on whether the potential surface is nearly symmetrical or unsymmetrical. In the highly unsymmetrical case, the potential curve is more clearly visualized as a function of r(DH). The geometries of the proton-transfer complex were optimized using the 4-31G and 3-21G basis sets unless otherwise specified. The energies were all then calculated at the MP2/4-31G* level.

Because of the complexity of the system, it is very expensive to perform geometry optimization for all degrees of freedom, even at the RHF/4-31G and RHF/3-21G levels. Fortunately, some degrees of freedom, for example, the bond length of ligand water and their orientations, or the geometries of the imidazole molecule, have small or negligible effects on the proton-transfer energy surface. Thus, it is convenient to optimize these degrees of freedom once and keep them fixed afterward. These approximations will be discussed quantitatively later when the proton-transfer energy surfaces are presented.

Before any complex proton-transfer potential surface is calculated, however, it is important to validate the accuracy of the *ab initio* methodology. To this end, the well-studied $H_5O_2^+$ system, the symmetrical nucleophilic substitution of S_N2 reactions, and several torsional barrier calculations were chosen as test cases with good success. In the interests of brevity, all of these results are not presented here, but they are available by contacting the authors directly. Only the results for the proton-transfer barrier in the $H_5O_2^+$ complex are described here as they are directly relevant to the present work.

Proton Transfer in the $H_5O_2^+$ Complex. The geometries were optimized using RHF/4-31G and RHF/3-21G, while the energies were calculated at the MP2/4-31G* level. The RHF/4-31G and RHF/3-21G calculations give almost identical results (within 0.1 kcal/mol), so the differences can be neglected. The calculated *ab initio* potential surface

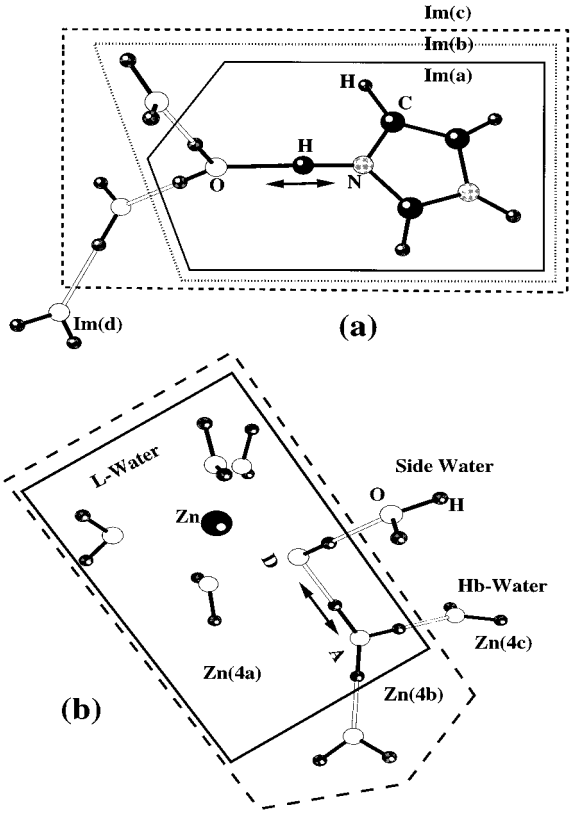

Figure 1. (a) Dehydration direction proton transfer complex under various situations: Im(b), Im(c), and Im(d) with 0, 1, 2, and 3 assisting ligand or secondary water molecules, respectively, as shown by the water molecules included within the various boxes. (b) Hydration direction PT transfer for Zn(4a), Zn(4b), and Zn(4c) with 0, 1, and 2 assisting ligand water molecules. These ligand water molecule are referred to as hydrogen-bonded water, or "Hb water". The water molecules around the Zn^{2+} ion are referred to as ligand water, or "L-water".

agrees very well with that of Ojamäe et al.,[29] in which a large correlation consistent pVTZ basis set with augmented diffuse functions on oxygen[30] was used. More importantly, the proton-transfer barrier heights are within 0.25 kcal/mol for various important R(O−O) distances (e.g., 2.6 and 2.8 Å). The accuracy of the present *ab initio* methodology for this system is important for the results relevant to the CA enzyme reported later.

Proton-Transfer Energy Surfaces

1. Dehydration Direction (Histidine Side) Proton Transfer. Proton transfer in CA in the dehydration direction is thought to consist of a proton transfer from a protonated His-64 group to Zn-bound water through a water bridge. Here, several cases of proton transfer in this direction are studied as shown in Figure 1a. Histidine is represented by an imidazole molecule, and the proton is transferred from the imidazole cation to the adjacent H_2O molecule.

Proton Transfer without Ligand Water Molecules. The proton-transfer energy surface for complex Im(a) [Figure 1a] is shown in Figure 2a. The potential surface is represented as a function of r(NH) since the surface is highly asymmetrical. The curves are essentially repulsive for the three R(N−O) distances studied, which means the product hydronium ion H_3O^+

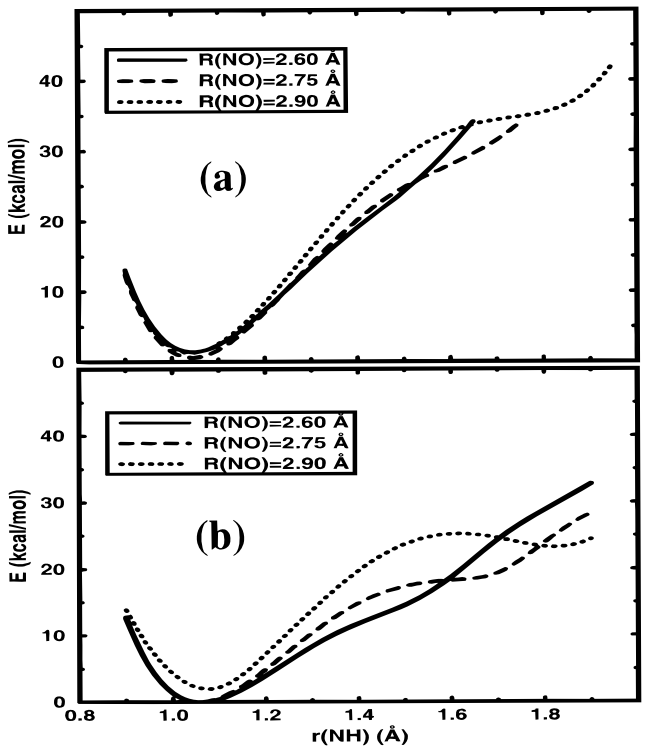

Figure 2. Proton-transfer energy surface for the $[Im\cdots H\cdots H_2O(H_2O)_n]^+$ complex with $n = 0$ and 1 for panels (a) and (b), respectively, at three N···O separations: R(N−O) = 2.6, 2.75, and 2.9 Å. These correspond to the Im(a) and Im(b) configurations, respectively, in Figure 1a. The surface in the first case gives a proton-transfer barrier larger than 35 kcal/mol. With addition of one hydrogen-bonded ligand water molecule for the Im(b) configuration, the barrier decreases by around 15 kcal/mol. This effect is due to a change of electrostatic interaction between ligand water and the proton-transfer complex in the process of proton transfer as shown in Figure 1a.

Table 1. A Comparison of the Proton and Zn^{2+} Affinities for Three Molecules: H_2O, NH_3, and Imidazole[a]

molecule	proton affinity	Zn^{2+} affinity
H_2O	170.7	95.9
NH_3	211.2	120.4
imidazole	238.5	162.7

[a] The values are obtained from *ab initio* MP2/6-311++G(2d,p) calculations. The LANL2DZ basis is used for the Zn^{2+} ion. The energies are in kilocalories per mole.

is never stabilized even at R(N−O) = 2.9 Å. At large N···O separation, the barrier height will be primarily the energy cost in breaking the N−H bond which is 238.5 kcal/mol (cf. Table 1), while after the transfer of the proton and formation of H_3O^+, it is stabilized by the amount of the proton affinity of H_2O, i.e., 170.7 kcal/mol (cf. Table 1). Thus, the proton-transfer energy surface may be expected to be a double well when R(N−O) is large. As the water molecule approaches the imidazole cation, the barrier height decreases and the stabilization energy of H_3O^+ with respect to the relevant transition state also decreases. Figure 2a shows the situation where the transfer product is of higher energy than the "transition state". From the figure, it is expected that the PT energy barrier for this configuration of molecules will be greater than 35 kcal/mol.

One Ligand Water Molecule Assisting Proton Transfer. With one hydrogen-bonded ligand water molecule added to the previous complex (Im(b) in Figure 1a, the proton-transfer energy surface in Figure 2b becomes less endothermic. At R(N−O) = 2.9 Å, the product H_3O^+ is slightly stabilized with repect to

(29) Ojamäe, L.; Shavitt, I.; Singer, S. J. *Int. J. Quantum Chem.: Quantum Chem. Symp.* **1995**, *29*, 657.

(30) (a) Woon, D. E.; Dunning, T. H. *J. Chem. Phys.* **1993**, *98*, 1358. (b) Kendall, R. A.; Dunning, T. H. *J. Chem. Phys.* **1992**, *96*, 6796. (c) Dunning, T. H. *J. Chem. Phys.* **1989**, *90*, 1007.

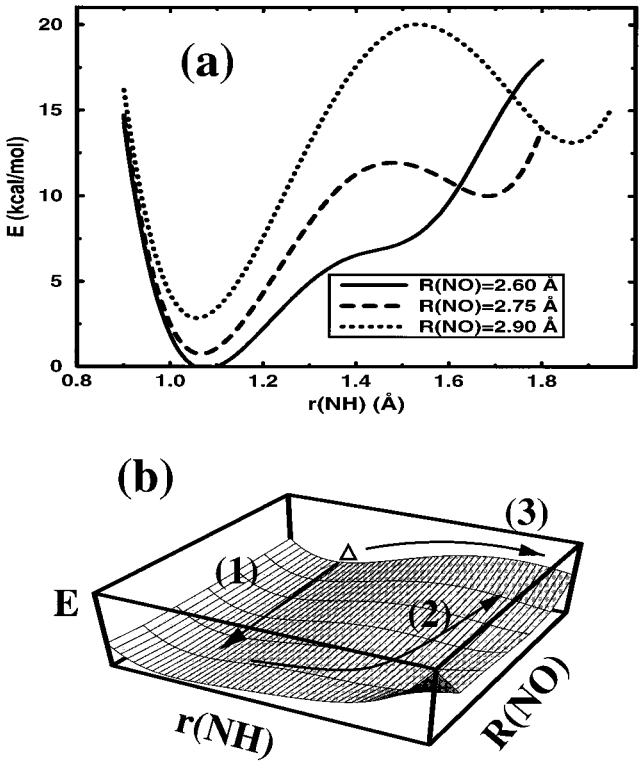

Figure 3. (a) The same potential surface as in Figure 2 except that there are now two ligand water molecules assisting the proton transfer, i.e., the Im(c) configuration in Figure 1a. The proton-transfer barrier is decreased by 10−15 kcal/mol compared to that in Figure 2b. (b) A schematic representation of the 3-D PT energy surface. There are two distinct channels that the proton can follow to get over the barrier starting from a typical configuration (indicated by the triangle): one is from route (3) (this would be significant when donor−acceptor motion is slow); the other is route (1) + (2), which arises from a cooperative behavior between the D−A motion and the proton motion. The realistic situation will likely be between the two limits.

the transition state. In this case, one might expect that the proton-transfer barrier will be around 20−25 kcal/mol, where a metastable proton-transfer product is obtained at certain *R*(N−O) distances. Compared to the previous case, it is estimated that the proton-transfer barrier is decreased by roughly 15 kcal/mol. As will be seen in the charge distribution and energy component analysis in the next section, this is mainly due to the electrostatic interaction between the ligand water molecule and the proton-transfer complex.

Two Ligand Water Molecules Assisting Proton Transfer. As one more ligand water molecule is added [cf. Im(c) in Figure 1a], the proton-transfer barrier is further decreased as shown in Figure 3b. The transfer product is rather stabilized at *R*(N−O) = 2.75 Å, and there is a well-defined transition state. At this point, a proton-transfer barrier of around 12 kcal/mol is obtained.

The effect of a secondary ligand water molecule (two H bonds away from the proton acceptor), i.e., the Im(d) configuration in Figure 1b, is shown in Figure 4. At *R*(N−O) = 2.75 Å, the barrier is decreased by around 3 kcal/mol to be around 8 kcal/mol.

A question arises as to the operational PT barrier since different transition states are observed for different *R*(N−O) distances. If the N···O distance is fixed, then the proton-transfer barrier may be best characterized by the situation in which the barrier is rather high [cf. 3-D potential energy surface in Figure 3b. In this scenario, starting from a typical configuration as indicated by a triangle in Figure 3b, the proton must take route

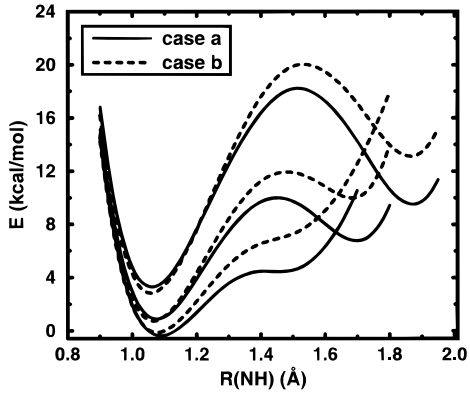

Figure 4. Change of the proton-transfer energy surface as one secondary ligand water is added to assist the proton transfer: case a, one secondary ligand water is added; case b, no secondary ligand water. The addition of a secondary ligand water leads to a further decrease of the PT barrier by around 3 kcal/mol. The three curves are for *R*(N−O) at 2.90, 2.75, and 2.60 Å from top to bottom.

(3) to reach the product well. On the other hand, if the N···O motion is taken into account, then the proton-transfer barrier is modulated by the fluctuations in *R*(N−O) so that a pathway like (1) + (2) involving an inward fluctuation of the N···O distance can occur. This mechanism will be assumed. Since the N···O motion is relatively slow compared to the proton motion, it may also be assumed that the proton would have adequate time in the product well to undergo a second PT to another H-bonded (Hb) water molecule, rather than relax back to the reactant state from, e.g., the reverse of route (2) in Figure 3b. In the future, molecular dynamics simulations will be carried out to better characterize the overall mechanism.

2. Hydration Direction (Away from Zinc) Proton Transfer. Without any ligand molecules, such as the three histines in CA, Zn-bound water will spontaneously transfer a proton to adjacent water molecules due to the large repulsion from the Zn^{2+} ion. As ligand molecules are added around the Zn^{2+} ion, they compete with the Zn-bound water. Thus, it is expected that the PT energy surface is affected by both the hydrogen bond formation with the proton acceptor and the Zn ligand formation. Some early discussion existed regarding the number of ligands around the Zn^{2+} ion,[22] so it is interesting to see how the PT energy surface varies under different situations. It is also interesting to probe the effect of different ligands, such as H_2O, NH_3, and imidazole, since they possess different proton and Zn^{2+} affinities (cf. Table 1). Some of the situations for hydration direction proton transfer considered here are shown in Figure 1b. The Los Alamos effective core potential plus double-ζ basis set (LANL2DZ)[31] was used for Zn in both the geometry optimizations and the energy calculations.

Water Ligands around Zinc. Proton-transfer energy surfaces for complexes Zn(4a), Zn(4b), Zn(4c) [cf. Figure 1b] are shown, respectively, in Figures 5a,b and 6a. In this case, there are four ligand water molecules around the Zn^{2+} ion besides the Zn-bound water. Again, the effect of ligand water molecules around the acceptor water leads to a significant decrease in the transfer barrier. The decrease in the barrier height amounts to around 15 kcal/mol, similar to the dehydration direction proton transfer. Without the assistance of Hb waters, the barrier height is above 35 kcal/mol, with one assisting Hb water, it is around 20 kcal/mol, and with two assisting Hb waters, the PT barrier

(31) (a) Hay, P. J.; Wadt, W. R. *J. Chem. Phys.* **1985**, *82*, 270. (b) Wadt, W. R.; Hay, P. J. *J. Chem. Phys.* **1985**, *82*, 284. (c) Hay, P. J.; Wadt, W. R. *J. Chem. Phys.* **1985**, *82*, 299.

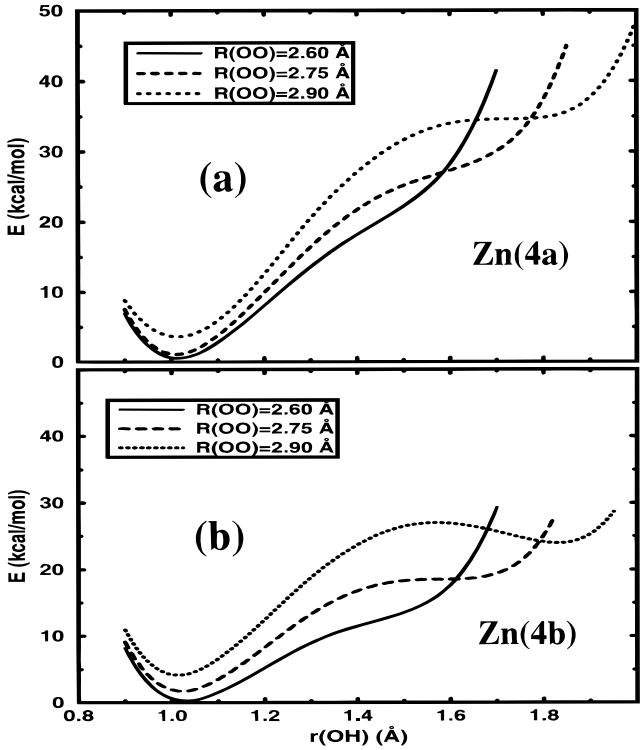

Figure 5. Proton-transfer energy surface for the $[(H_2O)_4Zn^{2+}\cdot H_2O\cdots H_2O(H_2O)_n]$ complex with $n = 0$ and 1 for (a) and (b), respectively, at three R(O−O) distances. Again the PT barrier decreases by an amount around 15 kcal/mol in going from $n = 0$ to 1 Hb-water.

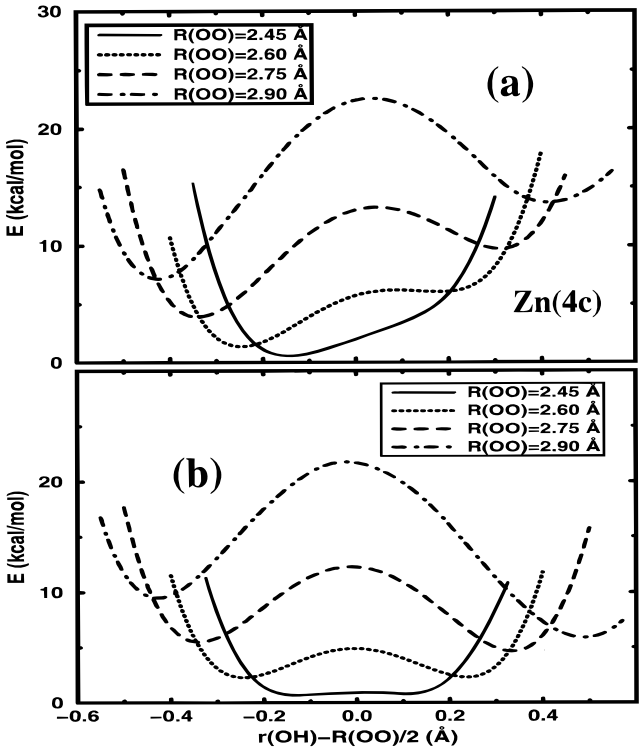

Figure 6. Proton-transfer energy surface for the $[(H_2O)_nZn^{2+}\cdot H_2O\cdots H_2O\text{-}(H_2O)_2]$ complex with $n = 4$ and 3 for panels (a) and (b), respectively, at four R(O−O) distances. The proton transfer in case (b) is almost spontaneous.

is decreased to around 5−10 kcal/mol at the point where the PT product starts to be stabilized.

With $n = 3$ water molecules around the Zn^{2+} ion, the Zn-bound water receives less competition from the ligands. Hence, the proton feels more repulsion from the Zn^{2+} ion. The corresponding PT energy surface is shown in Figure 6b. In this case, the proton transfer is spontaneous: the PT product is of lower energy than the reactant.

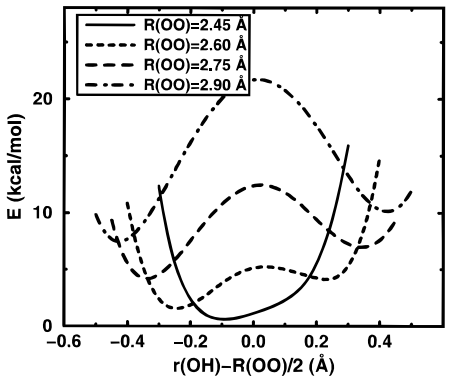

Figure 7. Proton-transfer energy surface as in Figure 6b except that three H_2O ligands around the Zn^{2+} ion are replaced by NH_3 molecules. The NH_3 ligands give a more repulsive surface than the H_2O ligands. This is rationalized by the difference in the Zn^{2+} affinities for the two ligands.

Ammonia Ligand Molecules around Zinc. Replacing the three H_2O molecules with three NH_3 molecules around the Zn^{2+} ion leads to an increase in the proton-transfer barrier (cf. Figure 7). This can be seen by examining the distance between the Zn^{2+} ion and the proton donor oxygen. As the NH_3 has a larger Zn^{2+} affinity (Table 1), the Zn^{2+} ion is pulled further away from the proton donor. As a result, the proton-transfer barrier increases. Furthermore, one expects the barrier will then increase even more as the ligand molecules are replaced by imidazole molecules because of their particularly strong Zn^{2+} affinity. This issue is explored below.

As opposed to the case of water ligands, the addition of a water molecule to the three NH_3 ligands only increases the PT barrier by around 1 kcal/mol at R(O−O) = 2.60 Å, so the potential energy surface is very similar to that in Figure 7. This is expected since the additional water shows less competition in the presence of the stronger NH_3 ligands. In the case of imidazole ligands, it is then further expected that the effect of water as a fifth ligand water will not have much effect on the proton-transfer potential surface. This is in fact confirmed in the following studies, and such a water ligand is not observed in the X-ray crystal structure.[13,15]

Imidazole Ligand Molecules around Zinc. In carbonic anhydrase, the Zn^{2+} ion is coordinated with three histidine residues. Thus it is far more realistic to represent the ligand histidines with imidazole molecules. The resulting PT potential energy surface is shown in Figure 8. Here, we have considered two ligand situations around the D−A complex. One situation [(1) and (2) in Figure 8] is the same as that in complex Zn(4c) in Figure 1b with three ligand waters replaced by imidazole groups; in the other situation [(3), (4), and (5) in Figure 8] an additional side water was added (cf. Figure 1). With three imidazole ligands around the Zn^{2+} ion, the PT energy barrier is around 20 kcal/mol, which is almost 15 kcal/mol higher than in the NH_3 ligand case. The Zn−O distance is around 0.15 Å longer than in the case of water ligands. With an additional side water, the PT barrier is increased by 10−15 kcal/mol, as expected, since the effect of side water is playing the opposite role of assisting the Hb water molecules. In CA, this side water position is occupied by Thr199 OG1,[13] but this group is expected to have a smaller effect on the barrier due to less charge on the OH group than in water.

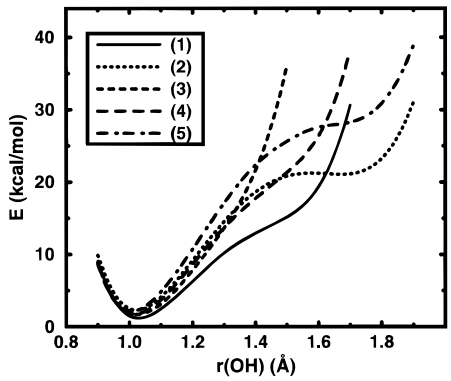

Figure 8. Cases (1) and (2): The proton-transfer energy surface is the same as that in Figure 6b except that three H_2O ligands around the Zn^{2+} ion are replaced by imidazole molecules, at R(O−O) = 2.6 and 2.8 Å, respectively. Cases (3), (4), and (5): same as (1) and (2), except that a side water shown in Figure 1b is added to the complex at R(O−O) = 2.60, 2.75, and 2.90 Å, respectively. This side water has a role opposite that of the Hb-waters in Figure 1b and leads to a larger barrier for hydration direction proton transfer.

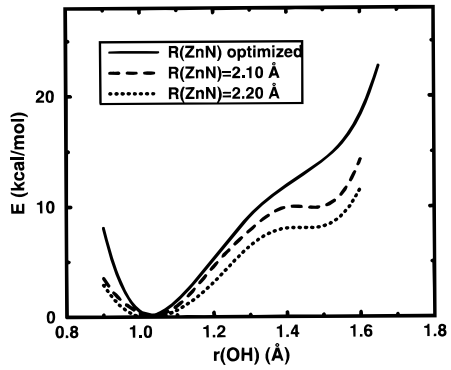

Figure 9. Potential energy surface for hydration direction proton transfer with three imidazole ligands around the Zn^{2+} ion at R(O−O) = 2.60 Å under three situations: (1) solid line, the distances between imidazole N atoms and the Zn^{2+} ion (R(Zn−N)) were optimized freely, in which case the equilibrium distance of R(Zn−N) is around 2.03−2.04 Å; (2) dashed line, R(Zn−N) is fixed at 2.10 Å; (3) dashed−dotted curve, R(Zn−N) is fixed at 2.20 Å. The proton-transfer energy barrier of the three cases dropped from more than 20 kcal/mol in (1) (see Figure 8) to ∼10 kcal/mol in (2) to ∼7−8 kcal/mol in (3).

In the above calculations, the geometries of imidazole ligand molecules were optimized through energy minimization. This may not be true in the native enzyme since the structure has been optimized by Nature for a particular function (in this case, proton transfer). As shown in the mutation studies of secondary ligands (GLU117, GLN92), the positioning of histidine ligands will give an entropy cost and this entropy may be compensated by the interaction with secondary ligands.[2] Mutation of the supportive ligands (GLU117, GLN92) will lead to a significant increase in the zinc dissociation constant, thus illustrating the subtle nature of the Zn^{2+} ion coordination in CA. It is also expected that thermal fluctuations will lead to differences from the minimal energy structures. Thus, the effect of the imidazole ligands on the PT barrier may differ in important ways from the calculations reported above.

Since the crucial effect of the ligands on the PT barrier arises from the distance from the Zn^{2+} ion, the PT barrier was studied for different R(Zn−N) distances. The resulting potential for three imidazole ligands with R(Zn−N) fixed at 2.10 and 2.20 Å is shown in Figure 9. Here only the situation for R(O−O) = 2.6 Å is shown. It is observed that the PT barrier decreases from ∼20 to 10 to 7−8 kcal/mol as R(Zn−N) goes from being

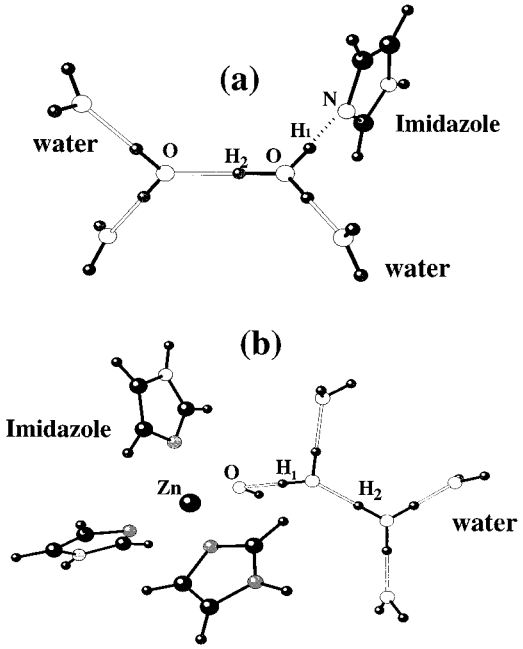

Figure 10. The second proton-transfer geometries for the dehydration (a) and hydration (b) direction proton shuttle. For the dehydration direction proton-transfer case, the distance $r(NH)_1$ between H_1 and the imidazole N atom was fixed. For the hydration direction case, the distance between O_1 and $H_1[r(OH)_1]$ was fixed so that the first proton would be stabilized in the product well.

freely optimized to being fixed at 2.10 and then 2.20 Å. This result confirms the conjecture regarding the effect of ligand distance on the PT barrier. The significance of these calculations will be discussed in the Discussion and Conclusions.

3. The Second and Further Proton Transfers. The transfer of a second proton in the water shuttle is also of fundamental importance to the overall proton-transfer energetics. In this case, the proton is transferred between two oxygen atoms. As the proton-transfer barrier between two water molecules is low to nonexistent depending on the O···O distance, one expects the barrier associated with the second PT to be low. Situations in both the dehydration [Figure 10a] and hydration [Figure 10b] directions have been considered. Since we are interested here in the PT surface after the first PT, the distance between the donor and proton in the first PT was fixed to make sure that the proton was stabilized in the product well.

For the dehydration PT direction, the donor−proton distance of the first PT [$r(NH)_1$] was fixed at three distances, 1.4, 1.6, and 1.75 Å. The corresponding second PT potential curves (Figure 11) show the interesting result that there is a strong dependence of the PT energy on the r(NH) distance. When $r(NH)_1$ = 1.75 Å, the PT is experiencing a low barrier of not more than 2−3 kcal/mol, while the barrier is increased to more than 10 kcal/mol when r(NH) is around 1.4 Å.

The hydration PT direction gives similar results. Here two cases were considered: one for which $r(OH)_1$ was fixed at 1.55 Å and the other for which $r(OH)_1$ was fixed at 1.65 Å, both with R(O−O) = 2.6 Å for the second PT. The latter barrier is increased from ∼2 kcal/mol when $r(OH)_1$ = 1.65 Å to ∼4 kcal/mol when $r(OH)_1$ = 1.55 Å. As opposed to the dehydration PT direction, the second PT transfer in this case is somewhat lower (∼1−2 kcal/mol when R(O−O) = 2.6 Å). This effect might be the result of repulsion from the Zn^{2+} ion. In general, considering the factors which influence the second PT, the overall proton-transfer picture appears to be a rather complicated

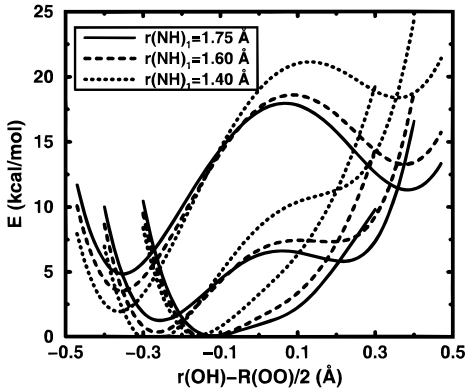

Figure 11. The second proton-transfer energy surface in the dehydration direction under three different $r(NH)_1$ distances and three different O···O separations: 2.4, 2.6, and 2.8 Å from bottom to top. One immediate conclusion is that, in order for the second proton transfer to happen, the $r(NH)_1$ distance in the first transfer must be be large. This means that the N···O distance will be correspondingly large.

one. This issue will be discussed further in the Discussion and Conclusions.

The third PT in the water shuttle for the hydration direction will be the opposite of the first PT in the reverse direction. Thus, it will happen spontaneously as the PT potential energy surface shows. One question then follows: What is the activation energy for the whole PT process from Zn-bound water to His-64 or vice versa? Is it determined solely by the first PT barrier because the first PT is the rate-determining step? Or is it the summation of barriers of all PTs? Or do the PTs happen at the same time, which means it is a concerted process and hence the barrier is the one related to the concerted reaction? This is a very difficult question to answer since there are many factors involved. In principle, one has to consider the motion of three protons, which means at least a potential surface as a function of three proton-transfer reaction coordinates is needed. In the present paper, we will not try to answer this question in detail; rather we will provide some general conclusions regarding the possible PT mechanisms and defer explicit dynamical studies to the future.

4. Discussion of Approximations. Several approximations have been used in the present calculations, and their effects on the energy surface are as follows.

(1) The imidazole rings are held fixed: Optimizations at selected points such as at the double well and barrier regions show that this effect is within 0.5 kcal/mol.

(2) In some situations, the orientation of ligand molecules around the Zn^{2+} ion is held fixed to ensure that they will not form any bond with the other proton-transfer species. This type of bond is certainly not realistic. Optimization on selected points shows the effect is less than 0.8 kcal/mol.

(3) In the calculations, the angle D···H···A is assumed to be 180°. The charge-transfer probability will depend on the wave function overlap between charge-transfer groups. Thus it is expected that not much bending of, e.g., the O···H···O angle will happen in the proton-transfer process. In the $H_5O_2^+$ case, the optimization of the O···H···O angle shows an effect of less than 0.1 kcal/mol, which is essentially negligible.

(4) The bond length of the ligand molecules (e.g. O···H in water and N···H in NH_3) have been fixed during the proton transfer process. These have a similarly negligible effect on the potential energy surface.

Charge Distribution and Energy Component Analysis

The proton-transfer process involves a gradual breakage of the D−H bond and a corresponding gradual formation of the A−H bond, where "D" and "A" are the proton donor and acceptor species, respectively. During the process, the electrostatic interactions with the surrounding residues and solvent molecules will change as well. Thus, it is important to probe how the charge distribution changes along the proton-transfer coordinates and how the bonding and certain key electrostatic energies change.

The Merz−Kollman/Singh electrostatic potential-derived charges[32] for several functional groups in the $[Im\cdots H\cdots H_2O\text{-}(H_2O)_2]^+$ complex were calculated. It was observed that the proton charge remains around 0.4 electron charge throughout the transfer process. Its change along the PT coordinate is rather small compared to the amount of charge transferred between the proton donor N and the acceptor O, which is around 0.4 electron charge of opposite sign. As expected, the charge for the ligand water group remains the same (around zero) throughout the transfer process. It seems clear that there are two stabilization effects due to the presence of ligand water. One is the electrostatic interaction between the ligand water and the transferred proton, while the other is the interaction between the ligand water and transferred charge.

The same calculations were carried out for several functional groups in $[(H_2O)_4Zn^{2+}\cdots H_2O(H_2O)]$. Again the proton charge remains almost constant close to 0.7 throughout the transfer process, while the transferred charge from acceptor to donor drops to around 0.25 electron charge. This change in transferred charge is compensated by the transferred proton charge and again leads to a stabilization effect around 15 kcal/mol from the ligand water molecules, the same as in the dehydration PT direction.

It is also interesting to probe the electrostatic interaction energy and bonding energy for the proton-transfer complex $[Im\cdots H^+\cdots H_2O(H_2O)_n]$ for $n = 0$, 1, and 2 shown in Figure 12. Even without any assistance from ligand water, the electrostatic interaction favors the formation of H_3O^+. As the number of ligand water molecules is increased, the PT product becomes more stabilized. Evidently, the stabilization energy is consistent with the decrease in PT energy barrier.

The bonding energy E_b in Figure 12b is calculated by subtracting the electrostatic interactions from the previous calculated potential surfaces. The energies now are normalized to the same level for the three different ligand situations. Under three different situations, it is striking that the bonding energies are largely the same despite the distinct differences in electrostatic interactions. This occurs since the bonding energy gives the energy associated with the process of donor−proton bond breaking and acceptor−proton bond formation, which is not greatly affected by small electrostatic perturbations. Here, it is seen that the bonding energy difference in reactants and products is around 60−70 kcal/mol, which is consistent with the difference in proton affinity of ∼67 kcal/mol.

Earlier PT potential surface calculations on the C_2 symmetry $H_9O_4^+$ complex are almost exactly the same as for $H_5O_2^+$.[34] The reason resides in the fact that the charge distribution is almost the same for both situations. Then, as a result of symmetry, the electrostatic interactions due to the ligand molecules are almost the same at any point of the proton-transfer process. This is only true for symmetrical proton transfer. For

(32) (a) Besler, B. H.; Merz, K. M., Jr.; Kollman, P. A. *J. Comput. Chem.* **1990**, *11*, 431. (b) Singh, U. C.; Kollman, P. A. *J. Comput. Chem.* **1984**, *5*, 129.

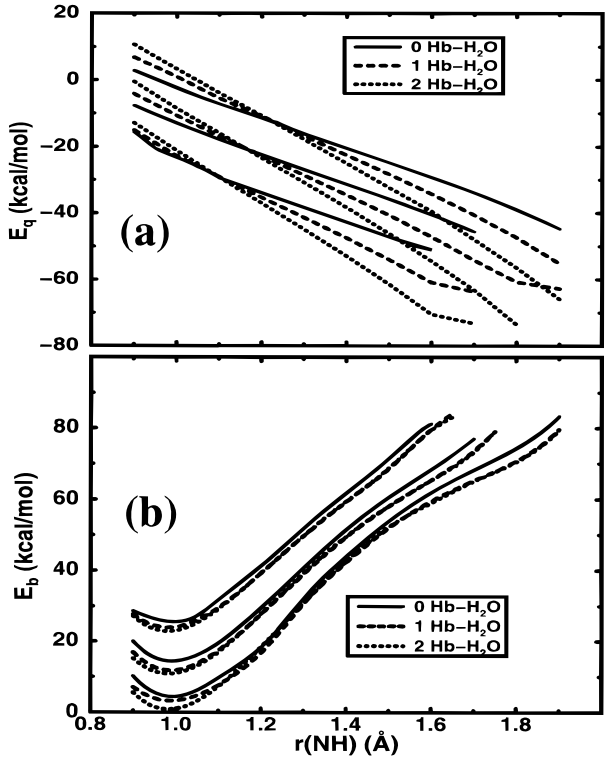

Figure 12. (a) Change in the electrostatic interaction in the process of proton transfer for the [imidazole···H^+···$H_2O(H_2O)_n$] complex at three different R(N−O) distances (2.6, 2.75, and 2.9 Å from top to bottom) and (1) $n = 0$, (2) $n = 1$, and (3) $n = 2$. This figure shows the proton transfer is favored by electrostatic interactions. The assistance from each ligand water molecule lowers the barrier by ∼10−15 kcal/mol. (b) The same as (a), but for the bonding energy contribution.

unsymmetrical proton transfer, the electrostatic stabilization due to ligand water molecules will not be the same, since the charge distribution is not symmetrical in the PT coordinate.

Further Considerations

There are several factors that may affect the proton-transfer barrier. First, variations of the residues which are coordinated to the relevant species in the proton-transfer complex may have a significant consequence on the PT energy surface. The effects of such mutations will be the subject of a forthcoming study. Second, one may argue that the protein electrostatic environment might influence the proton-transfer surface. To probe this effect, one can treat the protein environment as a dielectric continuum. As the dielectric constant of a typical protein environment is around 2−4, it is important to see how large the effect is on the proton-transfer barrier from self-consistent reaction field (SCRF) calculations. The proton-transfer energy surface for the $H_5O_2^+$ complex was therefore calculated for different surrounding dielectric continua. The proton-transfer barrier at certain R(O−O) distances was found to change somewhat, though not a great deal. For example, at R(O−O) = 2.6 and 2.8 Å, respectively, changes of ∼1.0 and 1.5−2.5 kcal/mol were observed when $\epsilon = 2-4$. This dielectric effect results from the stabilization of PT reactant and product by the surrounding medium. In this case, the charge is evenly distributed at the transition state and biased to one end in the reactant and products.

The surrounding dielectric effect on the model for dehydration direction proton transfer in CA was also studied. Here, the proton-transfer barrier was decreased by around 1 kcal/mol at R(N−O) = 2.75 Å, while the proton-transfer product was stabilized by around 2 kcal/mol. In the case of hydration direction proton transfer, the reactant was slightly more stabilized by the medium than the product, which increased the PT barrier by ∼1 kcal/mol.

Another factor which may have an effect on the PT barrier will be quantum zero point energy (ZPE). Due to its zero point energy, the proton should experience a lower barrier than expected classically. As the OH vibrational frequency may lie between 1300 and 2000 cm^{-1}, a reasonable estimate for the effect of ZPE may be around 1.5 kcal/mol. Another possibly important quantum effect is tunneling. The proton de Broglie wavelength is around 0.4 Å at room temperature,[33] which is comparable with the proton-transfer length scale. Quantum molecular dynamics simulations on proton transfer in water[33] show that the quantum effect eliminates the PT barrier between two water molecules.

Discussion and Conclusions

From the results presented in the previous sections, some conclusions can be drawn.

First, it is found that without the assistance of nearby water molecules, the proton-transfer barrier is too high in comparison with the experimental values. This fact alone points to the importance of H bond network formation in the active site. It is worth noting that this feature has also been suggested by site-directed mutagenesis studies,[17] where the pK_a of the Zn-bound water changes significantly when some residues around the active site are mutated. For example, mutation of T199 in CA II can lead to a change to 1.5 pK_a units; mutation of V143 inside the hydrophobic pocket to a series of different residues leads to a change of pK_a up to 1.6 pK_a units.[17] These changes can be ascribed to possible changes in the H bond network formation around the active site.

Second, the PT barrier in the hydration direction strongly depends on the nature and distance of the ligands around the Zn center. If the freely optimized (energy-minimized) imidazole molecules are taken as the ligands (i.e., R(Zn−N) ≈ 2.03−2.04 Å), the barrier is higher than 20 kcal/mol even after an estimation of the zero point energy. If the effect of the Thr199 OG1 group is taken to be similar to that of the side water in Figure 1b, the barrier height is estimated to be 25−30 kcal/mol. Thus, it seems that this result does not agree with the fact that Zn-bound water has a pK_a around 7, even considering the possible errors intrinsic to the method that have been used in the calculations. However, it has been shown that the Zn−O and Zn−N(His) distances are crucial in determining the PT barrier. When the Zn−N distance is small, the O atom is pushed away from the Zn^{2+} ion and the barrier becomes high; on the other hand, if the His ligands are not as tightly bound, e.g., such as in the cases where R(Zn−N) is fixed at larger values, the energy barrier will be lowered considerably (cf. Figure 9) to be in better agreement with experiment. To obtain a good estimate of the hydration direction transfer barrier, it is then essential to know the distances between the Zn^{2+} ion and histidine ligands to around 0.05 Å. Unfortunately, X-ray diffraction experiments do not yet have enough precision to provide this information. From ref 14, the R(Zn−N) distances give an average of around 2.2−2.3 Å for the protonated state of Zn-bound water, with an standard deviation of around 0.2−0.3 Å. This fact places added emphasis on the need for accurate calculations for such systems as CA in order to better understand the PT mechanism.

(33) Lobaugh, J.; Voth, G. A. *J. Chem. Phys.* **1995**, *101*, 409.

It should be noted that molecular dynamics simulations have been used to provide an estimate of the Zn−His distances in CA. In these simulations, the effects of protein constraints and thermal fluctuations can also be addressed. With an appropriate choice of ligand bonding parameters as derived from *ab initio* studies, it was found that the average distance between the Zn^{2+} ion and the histidine residues is ∼2.10−2.15 Å (cf. ref 44 for details). So the hydration direction proton-transfer barrier is estimated to be around 10 kcal/mol, which agrees well with experiment.[6] Thus, Nature may have selectively determined the binding character of the His ligands such that the Zn^{2+} ion is perfectly bound in order to have the requisite biological activity. This situation is in some ways similar to the case of CA III, whose turnover rate is 300-fold smaller than that of CA II. In CA III, some important residues close to the Zn-bound histidines are different from those in CA II. Modification such as Ile198 in CA II to Phe198 in CA III leads to dramatic changes in the Zn-bound water pK_a and catalytic activity.[34]

The picture of the first PT step is also intrinsically coupled to second and third PTs in the water chain. Depending on the *R*(DA) distance of the first PT, which determines the first PT barrier, the second PT barrier also varies. The first PT product well becomes deeper as the D···A distance becomes larger, which means the product becomes more stable and thus has more residence time, so the second PT can occur, which likely happens at small D···A separations for that step. Similarly the third and second PTs are also correlated. This correlation suggests a pattern for stepwise proton transfers: in order for the next proton transfer to happen, the D···A distance of the previous one must become elongated, while that of the present one must be shortened, both occurring through vibrational fluctuations. The presence of His-64 in CA provides a double well "sink" for the eventual end to this shuttle process.

For the dehydration direction PT barrier, the present calculations estimate it to be around 8−10 kcal/mol. This result is in good agreement with the experimental value.[12] Certainly, a more trustworthy result must take into account the exact protein environment, fluctuations, and the other effects discussed earlier, and such studies are underway. The present results also support the notion that a matching pK_a requirement for the Zn-bound water and His-64 is crucial to the efficient PT transfer in both directions.

In light of the present results, one can conclude that, in order for the His-64 PT channel to be efficient, at least a third water molecule connecting the Zn-bound and His64-bound water must exist as a transient structure. Since such hydrogen bond formation will cost free energy, the free energy barrier involved in this process is of great interest. The Marcus theory analysis by Silverman et al.[9] on the dehydration direction PT transfer gives an estimate of the work term of 10.0 ± 0.2 kcal/mol, which may include the hydrogen bond formation free energy. Since no direct experimental result is available regarding the H bond formation, it will be essential to study this through computer simulations using free energy perturbation or umbrella sampling techniques.[35]

Despite an extensive experimental effort in studying the mechanism of proton transfer in carbonic anhydrase, the mechanism and dynamics of the proton shuttling have not yet been resolved. This state of affairs has motivated the present theoretical effort. This effort will continue in the future through the determination of more accurate potential energy surfaces and molecular dynamics simulations, including the effects of proton quantization.

Acknowledgment. We thank Professors David Silverman and David Christianson for their critical comments and Drs. Lars Ojamäe and Sanjay Chawla for many helpful and stimulating discussions. This work was supported by the National Institutes of Health (Grant GM-53148).

JA973397O

(34) LoGrasso, P. V.; Tu, C. K.; Jewell, D. A.; Wynns, G. C.; Laipis, P. J.; Silverman, D. A. *Biochemistry* **1991**, *30*, 8463.

(35) Lu, D.; Voth, G. A. Manuscript in preparation.